Water Science & Technology

IWA PUBLISHING

Water Science & Technology Vol 84 No 4, 865 doi: 10.2166/wst.2021.284

Determination of chemical oxygen demand in mixed organic solution by Ti/TiO_2 nanotube array electrode method

Xiaojiao Li[a,b], Lan Wang[a] and Linshan Wang[a,*]

[a] Department of Chemistry, Northeastern University, Shenyang 110819, China
[b] State Key Laboratory of Rolling and Automation, School of Materials Science and Engineering, Northeastern University, Shenyang 110819, China
*Corresponding author. E-mail: lswang@mail.neu.edu.cn

ABSTRACT

Chemical oxygen demand (COD) is a significant parameter for analyzing water quality. However, the detection methods still suffer from the problems of secondary pollution, use of harmful substances, complicated operations, etc. To trace these problems, a Ti/TiO_2 nanotube array (NTA) electrode was successfully prepared in this work by the secondary anodic oxidation method. The prepared electrode was used to determine the COD of single- and multi-component solutions (including aniline, rhodamine B, and potassium hydrogen phthalate). The Ti/TiO_2 NTA electrode exhibited higher electrochemical oxidation efficiency than the neat Ti one. The electrocatalytic reactions of the target organics on the electrode surface were confirmed to conform to the first-order kinetic process. Within a COD range of 5–150 mg/L, COD value was not only proportional to the anodizing current but also related to organic matter itself. The activation energies of electro-oxidation reaction of different substances differed from each other (An: 14.25 kJ/mol, RhB: 18.56 kJ/mol, and KHP: 35.32 kJ/mol), indicating the differences in their dynamic behaviors on the electrode surface. The related bias obtained for all successive measurements was below $\pm$ 5.8%. Therefore, we report a fast, effective, accurate, and well reproducible COD detection method that is feasible for both single-component and multiple-component organic solutions.

Key words: chemical oxygen demand, electrochemical method, multi-component solution, Ti/TiO_2 electrode

HIGHLIGHTS

- A Ti/TiO_2 nanotube array electrode was prepared by a secondary anodic oxidation method, a simple and rapid technique.
- The Ti/TiO_2 electrode exhibited high electrochemical performance. Its electro-oxidation kinetics conformed to first-order kinetics.
- For COD determination by the Ti/TiO_2 electrode, net current was affected by temperature, and types and ratios of organics, due to functional groups in the organics.

GRAPHICAL ABSTRACT

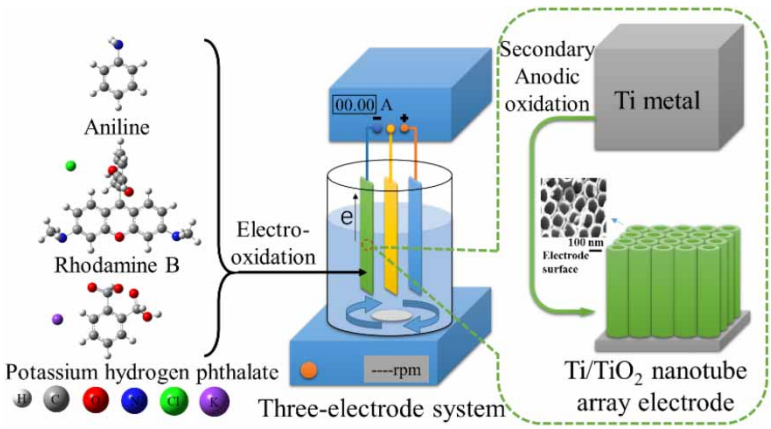

1. INTRODUCTION

Increasing water pollution has become one of the pressing global challenges, and makes environmental monitoring and control a global concern (Shannon *et al.* 2008; Ercin & Hoekstra 2014; UNESCO & UN-Water 2020). Chemical oxygen demand (COD) reflects the degree of contamination of water by reducing substances and is one of the most widely used indicators in the field of water-quality analysis such as wastewater effluent monitoring and taxation of wastewater pollution (Zheng *et al.* 2008). The potassium dichromate method, as the traditional COD method, is applied to evaluate the demand of oxygen required for the oxidative degradation of organic compounds. The conventional process of this method includes the complicated operation steps of catalytic oxidation, reflux, and titration. It requires 2–4 hours of operation time to achieve sufficient oxidation for COD determination, so it is difficult to apply for online monitoring or on-site evaluation (Li *et al.* 2006b; Ge *et al.* 2016). In addition, it also consumes some corrosive, expensive, and toxic chemicals such as H_2SO_4, Ag_2SO_4, Hg^{2+}, and $Cr_2O_7^{2-}$, leading to secondary pollution and high cost (Silva *et al.* 2009; Ge *et al.* 2016).

In past years, significant advances have been made for the accurate determination of COD values. However, the formidable challenge, still not solved comprehensively, is to develop a precise, rapid, and environmentally benign method for COD determination. Electrode technology measurement methods have been developed through electrocatalytic approaches using electrodes such as PbO_2 (Ai *et al.* 2004; Mo *et al.* 2015), Cu (Silva *et al.* 2009; Carchi *et al.* 2019), or Ti (Ge *et al.* 2016), to shorten the analysis time. Mo *et al.* reported a three-dimensional structured β-PbO_2-coated criss-crossing carbon fiber electrode for measuring COD values in wastewater (Mo *et al.* 2015). This electrode possessed a wide linear range of COD values (50–5,000 mg/L), high sensitivity, excellent reproducibility, and low cost. But this method was limited by the use of highly toxic heavy metal lead. Silva *et al.* demonstrated the feasibility of an electrochemical method using Cu electrodes to determine COD (Silva *et al.* 2009). In addition to low cost and simple preparation, the electrode has good stability for up to 15 days. However, the measurement time of 10–20 min was still not short enough and limited the development of this method. In addition, Carchi *et al.* prepared Cu/CuONf electrodes by covering Cu/CuO electrodes with Nafion (Nf) film (Carchi *et al.* 2019). The improved electrode measured the COD value more accurately and had a longer lifetime than the original Cu/CuO electrode, but sensitivity was reduced by about 15%. Compared with these methods, electrocatalytic approaches using Ti/TiO_2 electrodes are more promising, because of the superior oxidative abilities of TiO_2 and the short time required for analysis (Cheshideh & Nasirpouri 2017; Ramasundaram *et al.* 2017; Yi *et al.* 2019; Chen *et al.* 2020c). Moreover, TiO_2 nanomaterials are inexpensive, non-toxic, and environmentally friendly, and therefore have recently attracted interest for improving the catalytic degradation of various organic substances (Song *et al.* 2020). The main disadvantage of the Ti/TiO_2 electrode method in actual COD determination is that the electron/hole pairs generated in the discrete TiO_2 nanoparticles and the coated nanofilms are easy to recombine, resulting in low catalytic activity. This means a narrow dynamic working range and relatively poor reproducibility. For the COD determination using the electrochemical technique of Ti, Ge *et al.* developed a Ti/TiO_2 electrode using an anodizing method (Ge *et al.* 2016). The rapidity and accuracy of this method for monitoring COD values were confirmed. However, this study lacks research on diversified target solutions and only tested two single-component solutions of potassium hydrogen phthalate and phenol. Therefore, the research and analysis of Ti/TiO_2 electrode kinetics, the detection of diversified target solutions, and the development of electrodes are still of substantial value and far-reaching scientific significance within the working range of 5–150 mg/L COD value.

To deeply study the research, we had prepared a Ti/TiO_2 electrode with nanotube array (NTA) structure by the secondary anodic oxidation method. The preparation and characterization of the prepared electrode, the electrolysis kinetics of different organic substances on the electrode surface, and their application in COD determination of single- and multi-component mixed organic solutions are described in detail below.

2. MATERIALS AND METHODS

2.1. Experimental device

The experimental device consisted of an electrochemical workstation, a magnetic stirrer, an electrolytic cell, a working electrode, a counter electrode, and a reference electrode (Wang *et al.* 2020). The schematic diagram of the three-electrode system device is shown in Figure 1. In this work, the electrochemical workstation provided a stable current output. A prepared Ti/TiO_2 NTA electrode was used as the working electrode, and the area of the electrode immersed in the electrolyte is 100 mm^2. A Pt electrode or a porous graphite electrode was used as the counter electrode. The electrode spacing between the Ti/TiO_2 NTA electrode and the counter electrode is 2.5 cm. A saturated calomel electrode (SCE) was used as the

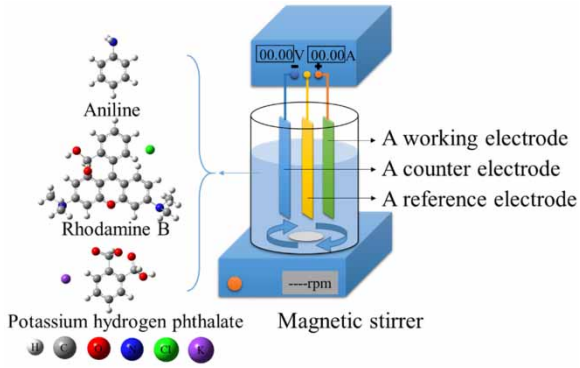

Figure 1 | Schematic depiction of the three-electrode system device.

reference electrode. In addition, a 0.1 mol/L Na_2SO_4 solution, as the supporting electrolyte, was stirred constantly in the electrolytic cell. However, for the electrochemical experiments, the final electrolyte was prepared by adding organic solutions into the supporting electrolyte (Chen *et al.* 2020b).

2.2. Materials

Titanium sheet (Ti sheet, 99.99% purity), nitric acid (HNO_3), hydrochloric acid (HCl), sodium hydroxide (NaOH), sulfuric acid (H_2SO_4, 98 wt%), aniline (An), and potassium hydrogen phthalate (KHP) were purchased from Sinopharm Chemical Reagent Co., Ltd, China. Ethylene glycol (EG) and ammonium fluoride (NH_4F) were brought from Shenyang Xinxing Reagent Factory, Shenyang, China. Hydrofluoric acid (HF) was from Shenyang Chemical Reagent Factory, Shenyang, China. Moreover, acetone, anhydrous ethanol, sodium sulfate (Na_2SO_4), and rhodamine B (RhB) were purchased from Damao Chemical Reagent Factory, Tianjin, China. For all purposes, Millipore water was applied.

2.3. Preparation of a Ti/TiO_2 NTA electrode

In this work, the Ti/TiO_2 NTA electrode was prepared by the secondary anodic oxidation method (Figure 2). A pure Ti sheet with a size of 15 mm × 60 mm × 0.4 mm was polished with 800, 1000, and 2000 grit abrasive paper to obtain a flat surface, and ultrasonically cleaned with acetone for 30 min, anhydrous ethanol for 15 min, and distilled water for 15 min, respectively. After that, the Ti sheet was etched with HF/HNO_3/H_2O solution (volume ratio = 1:2:5) for 20 s, and then dried at 80 °C.

Next, TiO_2 NTA was prepared on the surface of the Ti sheet by the twice anodization process. The pretreated Ti sheet was firstly anodized at 60 V for 30 min in EG electrolyte containing NH_4F (0.5 wt.%) and H_2O (3 vol.%), and a Pt electrode was used as the cathode. The oxide film formed on the surface was removed by ultrasonication in HCl (1 mol/L) for 5 min and

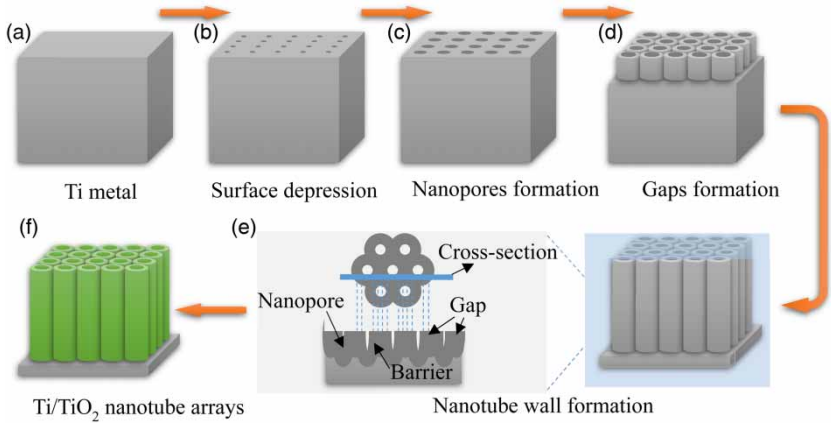

Figure 2 | Schematic diagram of the formation mechanism of Ti/TiO_2 NTA electrode prepared by anodic oxidation method (Tao & Tao 2008; Chen *et al.* 2020a).

then in absolute ethanol for 3 min. The as-prepared sheet was calcined without oxygen at 600 °C for 1 h. Then, the second anodization was performed for 1 h under the same condition as the first one. The sample was then rinsed with HCl (1 mol/L) for 3 min and then washed with acetone, absolute ethanol, and distilled water in order. Finally, the fabricated Ti/TiO_2 NTA electrode was calcined in a muffle furnace at 450 °C for 2 h (Tao & Tao 2008; Chen *et al.* 2020a).

2.4. Instrumental characterization

The structure and morphology of the Ti/TiO_2 NTA electrode were characterized by a field emission scanning electron microscopy (FE-SEM, SU8010, Hitachi Co., Tokyo). The crystal phase of the Ti/TiO_2 NTA was conducted *via* X-ray diffraction (XRD, Empyrean, PANalytical Co., The Netherlands), operating at 40 kV/40 mA using Cu-Kα radiation. In addition, linear scanning voltammetry (LSV) was used in electrochemical tests to measure the oxygen evolution potential of the electrode with 0.1 mol/L Na_2SO_4 electrolytes. The sweep speed was performed at 50 mV/s in the sweep voltage range from 0.0 to 3.0 V. A double beam ultraviolet-visible spectrophotometer (UV-vis, TU-1901, Beijing Puxi General Instrument Co., Ltd, China.) was used to analyze the solution absorbance.

2.5. Electrochemical measurement

For the electrode reaction kinetics, the three-electrode system device was applied for the experiments of electrocatalytic degradation (Figure 1). A porous graphite electrode was used as the counter electrode. The solutions of target organics, such as An, RhB, and KHP, were respectively added into the supporting electrolyte to obtain the final COD value of 50 mg/L (Chen *et al.* 2020b). The target organic solutions respectively degraded at different temperatures from 298 to 328 K. The degradation solutions were measured at the reaction time of 0–180 min. Using the UV-vis, the absorbances of An, RhB, and KHP were analyzed at the wavelengths of 479 nm, 230 nm, and 270 nm, respectively. Furthermore, the degradation rate (η) of the target degradation product at any time (t) can be obtained by the following equation:

$$\eta\ (\%) = \frac{A_0 - A_t}{A_0} \tag{1}$$

Among them, A_0 is the initial absorbance of the target organic solution, and A_t is the absorbance of the target degradation product at a degradation time t (Chen *et al.* 2020c; Zhang *et al.* 2020).

For the COD determination experiments, the same three-electrode system was used (Figure 1); the preparation method of the electrolyte was to add a standard solution with a known COD value to a 0.1 mol/L Na_2SO_4 solution. The working electrode voltage was controlled at 2–3.5 V (vs. SCE). The current was read after 60 s for stabilization. Compared with the conventional COD method, the Ti/TiO_2 electrode method has the advantages of short analysis time, low cost, non-toxicity, and environmental friendliness.

3. RESULTS AND DISCUSSION

3.1. Morphology characterization

Figure 3 shows an SEM image of the Ti/TiO_2 electrode surface with a nanotube array structure. The three-dimension TiO_2 nanotube array was prepared on a Ti sheet by the secondary electrochemical anodization. From the SEM image, the surface of the electrode is composed of a large number of ordered nanotubes, and the diameter of the inner hole is ~100 nm. The uniform TiO_2 nanotubes are high ordered in structure, well aligned with each other through the walls of the TiO_2 nanocrystalline tubes, and perpendicular to electrically conductive Ti substrates, thereby naturally forming a Schottky-type contact (Liu *et al.* 2009). Thus, due to the high surface area of TiO_2 NTA, the Ti/TiO_2 NTA electrode provided a large number of active sites thereby enhancing the adsorption capacity of organic pollutant molecules.

3.2. Composition analysis

The XRD characterization was conducted to further study the Ti/TiO_2 electrode material. Figure 4 shows the XRD diffraction pattern of the Ti/TiO_2 NTA electrode. It only shows the peaks of Ti and anatase TiO_2. The characteristic peaks of the anatase phase appear at 2θ of 26.35°, 37.78°, 48.08°, 53.92°, 55.11°, 62.73°, etc., corresponding to (101), (004), (200), (105), (211), (204), etc. crystal plane diffraction peaks of anatase phase (PDF card No. 21-1272 of the anatase phase TiO_2) (Daghrir *et al.* 2012, 2013). It indicates that the composition of the prepared nanotube array electrode is mainly anatase TiO_2.

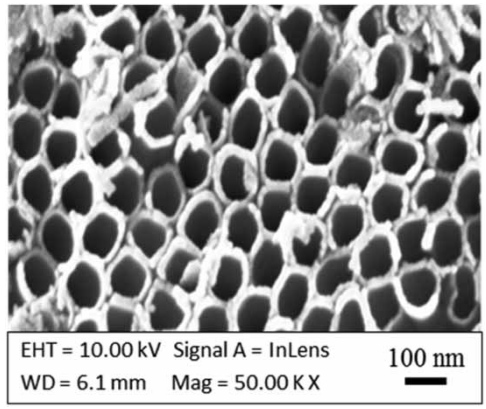

Figure 3 | SEM image of the Ti/TiO_2 NTA electrode.

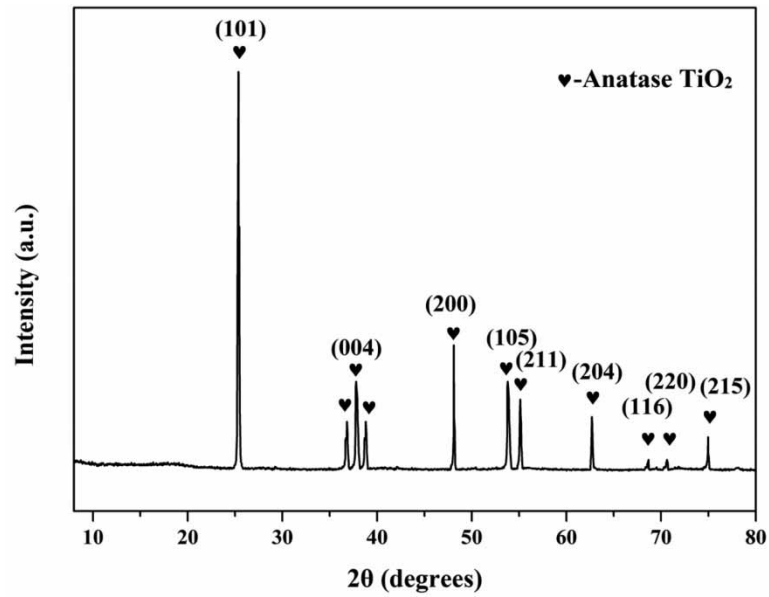

Figure 4 | XRD pattern of the prepared Ti/TiO_2 NTA electrode.

3.3. Electrochemical performance

The electrochemical tests were performed for the LSV curves (Figure 5) to analyze the properties of the test electrodes (Ti sheet and Ti/TiO_2 NTA electrodes) over the Pt electrode. As illustrated in Figure 5, the steady-state polarization curves of the Ti and the Ti/TiO_2 NTA electrodes have no oxidation peaks in the scanning range from 0.0 to 3.0 V. The oxygen evolution potential (OEP) of the prepared Ti/TiO_2 NTA electrode was approximately 2.48 V (vs. SCE), which was higher than that of the Ti one. It was ascribed to the higher surface area of the Ti/TiO_2 NTA electrode as compared to the Ti one, providing more active sites and enhancing the conductivity (Chen *et al.* 2020b, 2021). As the hydroxyl radicals (·OH) were reacted to O_2 to consume a large amount of active oxygen (Equations (2) and (3)), the oxygen evolution reaction (OER) was the main competitive side reaction against the oxidative degradation of organic pollutants. Therefore, compared with the Ti electrode, the Ti/TiO_2 NTA electrode with higher OEP can inhibit the occurrence of OER and increase the generation of ·OH (Equation (4)), thereby promoting the electrochemical oxidation efficiency of organic pollutants (Equation (5)) (Yu *et al.* 2014; Chen *et al.* 2020a; Xu *et al.* 2021). Thus, considering the OEP and oxidation overpotential, the prepared Ti/TiO_2 electrode was

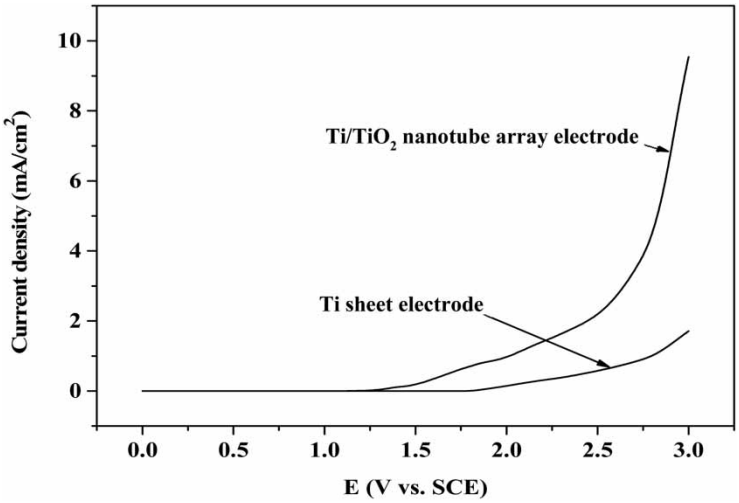

Figure 5 | LSV curves of the test electrodes in 0.1 mol/L Na_2SO_4 at a scan rate of 50 mV/s.

a satisfying choice for this work:

$$M(\cdot OH) \rightarrow 1/2O_2 + H^+ + e^- + M \quad (2)$$

$$M(\cdot OH) + H_2O \rightarrow O_2 + 3H^+ + 3e^- + M \quad (3)$$

$$M + H_2O \rightarrow M(\cdot OH) + H^+ + e^- \quad (4)$$

$$M(\cdot OH) + R \rightarrow CO_2 + H_2O + M \quad (5)$$

Herein, M represents the electrode material and R is for the representative organic pollutants (Saha *et al.* 2020; Chen *et al.* 2021).

3.4. Electrocatalytic degradation and electrolysis kinetics

The Ti/TiO_2 NTA electrode was used for the electrochemical degradation of the representative organics with an initial COD value of 50 mg/L by chronoamperometry. Figure 6 illustrated the curves of the degradation rates over different electrochemical oxidation time, in addition, the organic degradation on the Ti/TiO_2 NTA electrode at different temperatures were also in assessment. As the temperature increased from 298 to 328 K, the degradation effect of the organics (An, RhB, and KHP) increased within 180 min of electrolysis, reaching the maximum values of 97.6%, 96.8%, and 71.1% at 328 K, respectively. This was because higher temperatures were more likely to cause the organic pollutants to diffuse toward the electrode. Conversely, the degradation behavior of the different organic substances on the surface of the prepared electrode was different. In the electrochemical process, the degradation mechanism of organic pollutants can be divided into direct oxidation and

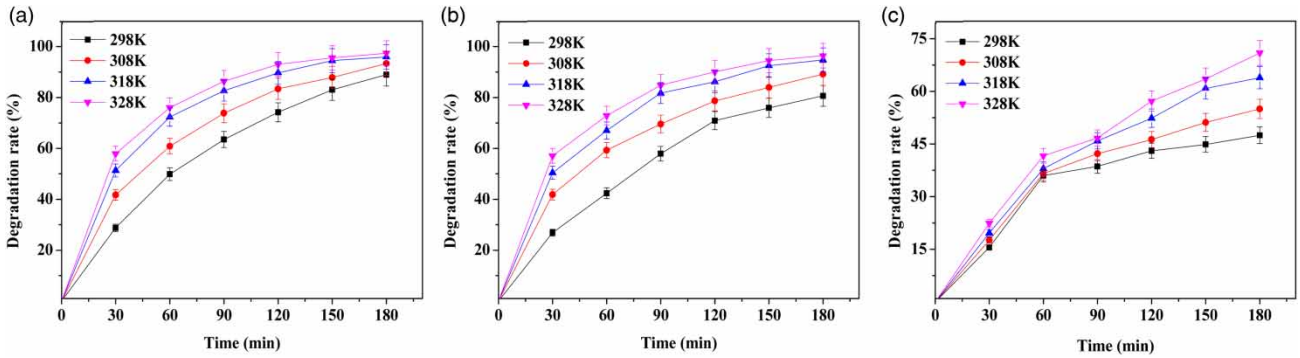

Figure 6 | Degradation rates of aniline (a), rhodamine B (b), and potassium hydrogen phthalate (c) over electrochemical oxidation time at different temperatures.

indirect oxidation. (Chen *et al.* 2021) Direct oxidation occurred through the direct transfer of electrons on the surface of the Ti/TiO_2 NTA electrode (Equation (4)) and was affected by temperature due to the degree of diffusion. Indirect oxidation referred to the process that organic pollutants were oxidized by ·OH (Equation (5)). It was affected by the type of organic matter (Garcia-Segura *et al.* 2018; Shao *et al.* 2019; Chen *et al.* 2021).

In addition, the reaction of the organics on the surface of the Ti/TiO_2 NTA electrode at different temperatures followed the quasi-first-order kinetic (Figure 7). Table 1 shows the related kinetic equations and parameters. The lnC of each representative organic decreased in proportion to the reaction time at temperatures from 298 to 328 K, and the correlation coefficients of the linear relationship were all above 0.99. This indicated that under the electrocatalytic reaction of the Ti/TiO_2 NTA electrode, the ·OH was stably produced. This was a free radical reaction process, which conformed to the assumption of the first-order kinetic process.

According to the reaction rate constant (k) in Table 1, the curves of lnk vs. the reciprocal of temperature (1/T) were plotted in Figure 8. Combined with the Arrhenius formula, the activation energies (Ea) of the electrocatalytic degradation of the representative organics (An, RhB, and KHP) were calculated to be 14.25 kJ/mol, 18.56 kJ/mol, and 35.32 kJ/mol, respectively. Activation energy represents the minimum energy required for the reaction of the reactant. The lower activation energies in this experiment compared with the activation energy of the general chemical reaction (60–250 kJ/mol) indicated that the electrochemical degradation was easier to carry out. Thus, the electrocatalytic degradation of KHP required the highest energy among the other target organics. This may be because some groups played a major role in the electrochemical degradation process, such as ·OH, hydroxyl group (-OH), amino group (-NH_2), amine group (-N=), etc. These groups can promote the decolorization of dyes and enhance the degradability of organic pollutants. Conversely, the molecular structure of RhB and KHP has inhibitory carboxyl groups (-COOH), and this inhibits the electrocatalytic degradation of -OH. In contrast, the inhibitory effect of KHP was the most obvious, and the catalytic degradation efficiency of An with the promoting group amino (-NH_2) was the highest. Therefore, the degradation reaction of An was the easiest to proceed with within this work.

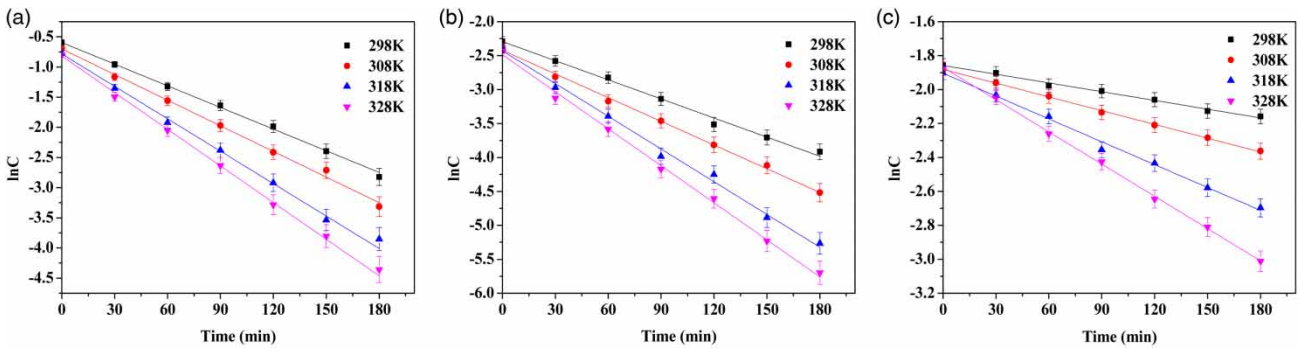

Figure 7 | The curves of the organic concentration C vs. the reaction time T for aniline (a), rhodamine B (b), and potassium hydrogen phthalate (c) at different temperatures.

Table 1 | Kinetic equations and correlation coefficients of the representative organics at different temperatures

Organics	Temperature (°C)	Linear regression equation (C, mol/L; t, min)	Kinetic constant k (min^{-1})	R^2
Aniline	25	$lnC = -0.0121 \cdot t - 0.5906$	0.0121	0.996
	35	$lnC = -0.0143 \cdot t - 0.6784$	0.0143	0.994
	45	$lnC = -0.0179 \cdot t - 0.7542$	0.0179	0.992
	55	$lnC = -0.0203 \cdot t - 0.7818$	0.0203	0.994
Rhodamine B	25	$lnC = -0.0094 \cdot t - 2.2862$	0.0094	0.992
	35	$lnC = -0.0119 \cdot t - 2.3732$	0.0119	0.990
	45	$lnC = -0.0163 \cdot t - 2.3869$	0.0163	0.990
	55	$lnC = -0.0185 \cdot t - 2.42811$	0.0185	0.991
Potassium hydrogen phthalate	25	$lnC = -0.0017 \cdot t - 1.8617$	0.0017	0.992
	35	$lnC = -0.0027 \cdot t - 1.8794$	0.0027	0.998
	45	$lnC = -0.0045 \cdot t - 1.9003$	0.0450	0.993
	55	$lnC = -0.00634 \cdot t - 1.8684$	0.0063	0.998

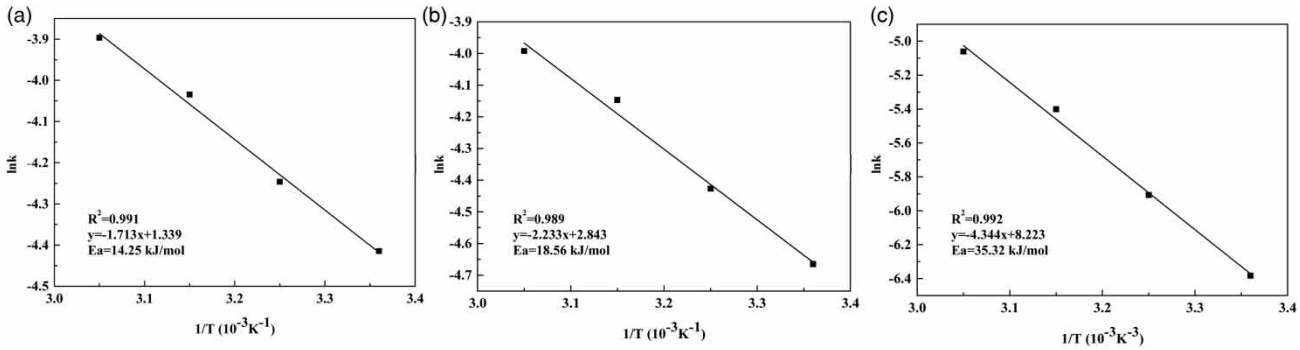

Figure 8 | The linear curves of lnk vs. 1/T for aniline (a), rhodamine B (b), and potassium hydrogen phthalate (c).

These indicated that the Ti/TiO_2 NTA electrode possessed a high catalytic degradation ability for the representative organics. The nanotube structure of the electrode provided a larger amount of adsorption and attachment points for the organic molecules in the solution, thereby improving the electrocatalytic degradation efficiency of the electrode. It was also attributed to the increased catalytic activity of the TiO_2 catalyst as the temperature increased.

In summary, in the electrocatalytic degradation and electrolysis kinetics using the Ti/TiO_2 NTA electrode method, the degradation rate of the organics (An, RhB, and KHP) increased with the temperature increased from 298 to 328 K in 180 min of electrolysis. In addition, it was revealed in Figure 7 that the lnC of each representative organic decreased in proportion to the time at test temperature from 298 to 328 K, and the correlation coefficients of the linear relationship were all above 0.99. Furthermore, the activation energies of the organic matter (An, RhB, and KHP) were calculated to be 14.25 kJ/mol, 18.56 kJ/mol, and 35.32 kJ/mol, respectively in the electrocatalytic degradation. Therefore, the electrochemical reactivity relationship of the target organics was An > RhB > KHP.

3.5. COD determination by Ti/TiO_2 NTA electrode method

3.5.1. COD determination of single-component solution

The net current over the COD concentration under different voltages was studied to investigate the linkage mechanism between electricity generation and the degradation of the organics.

As observed in Figure 9, in the range of 5–150 mg/L COD concentration, the current increased linearly with the increase of COD concentration for the single-component solution of the target organics. The related linear regression equations are shown in Table 2. In terms of the electricity generation mechanism, the used Ti/TiO_2 NTA electrode oxidized organic matter to produce electrons through electrochemical reaction (Equations (4) and (5)), thereby causing the current change (Zheng *et al.* 2008). Hence, higher COD concentration means that more organic matter can be degraded to generate more electrons, forming a higher current value. Xu *et al.* reported a similar view (Xu *et al.* 2021). Moreover, the net electrocatalytic current relationship of the organics was An > RhB > KHP under the same voltage. This indicated that the electrochemical reactivity relationship of the organics was An > RhB > KHP. Therefore, for a single-component solution, the net current (ΔI) not only increased in proportion to the COD concentration of each organic matter but also depended on the type of the organic matter. Conversely, the increase of the voltage significantly affected the enhancement of electrocatalytic degradation. This was attributed to the increase of the direct oxidation, producing more ·OH, which improved the efficiency of indirect oxidation and increased ΔI (Saha *et al.* 2020; Chen *et al.* 2021).

3.5.2. COD determination of multi-component solution

To further determine the relationship between COD concentration and oxidation current, the multi-component mixed organic solutions with known COD concentration were analyzed and measured by the electrochemical method. In this work, the representative organics were chosen, depending on their different functional groups, such as An with promoting groups (-NH_2), RhB, and KHP with inhibiting groups (-COOH), as shown in Figure 1. Moreover, these organics all have benzene rings in structure, which makes it easy to compare their electrochemical reactions.

For the two-component organic solutions, the linear curves of ΔI vs. COD and the related linear regression equations are shown in Figure 10 and Tables 3 and 4. As observed in Figure 10(a)–10(d) for the mixed solution of An/KHP, the current increased linearly with the increase in COD concentration with the range of 10–110 mg/L. Furthermore, in Figure 10(d)

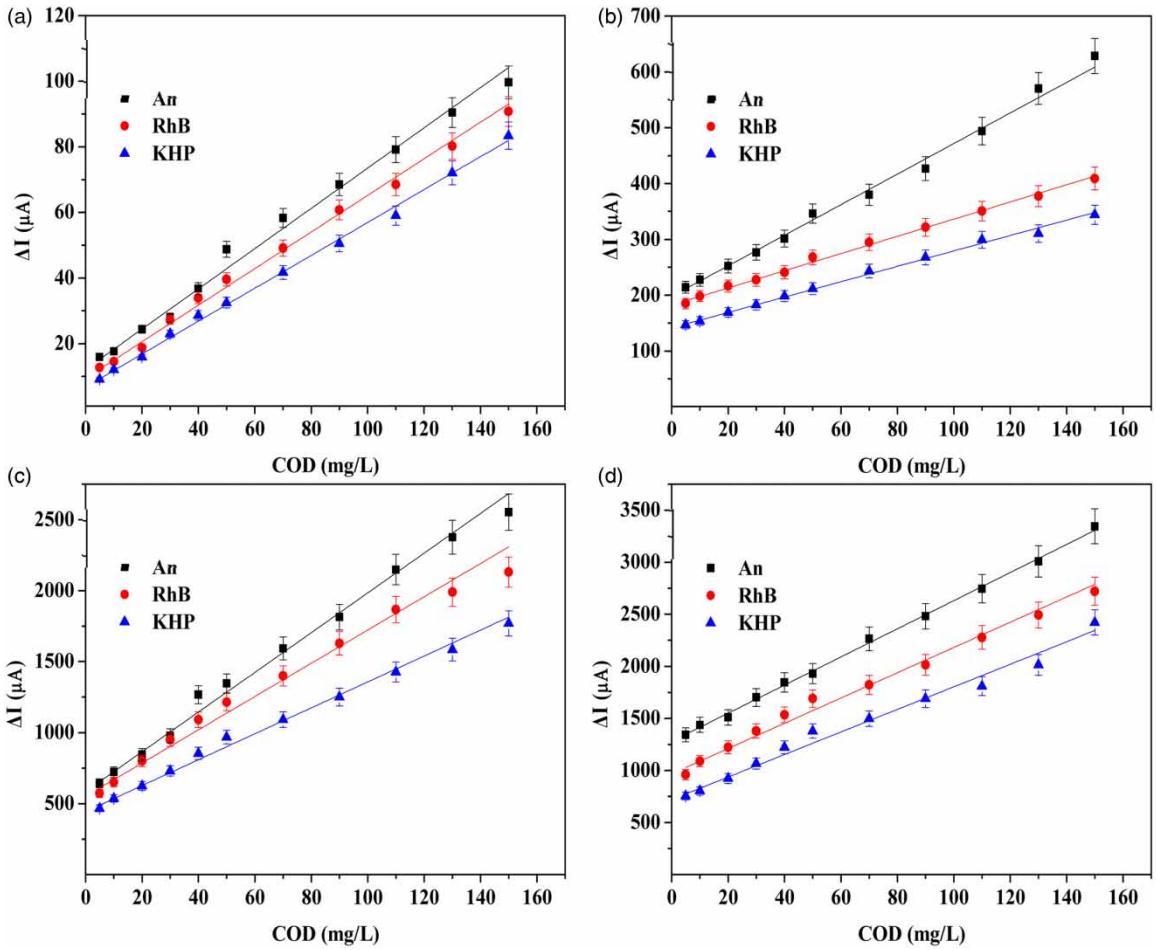

Figure 9 | The linear curves of the net current (ΔI) vs. the COD concentration of the representative organic pollutants at the voltages of 2.0 V(a), 2.5 V(b), 3.0 V(c), and 3.5 V(d), measured by the Ti/TiO_2 NTA electrode. An, RhB, and KHP stand for aniline, rhodamine B, and potassium hydrogen phthalate, respectively.

Table 2 | Linear regression equations of the net current (ΔI) and the COD concentration for the organic solutions of aniline, rhodamine B, and potassium hydrogen phthalate

	Aniline		Rhodamine B		Potassium hydrogen phthalate	
Voltage (V·vs. SCE)	Linear regression equation (ΔI, μA; COD, mg/L)	R^2	Linear regression equation (ΔI, μA; COD, mg/L)	R^2	Linear regression equation (ΔI, μA; COD, mg/L)	R^2
2	$\Delta I = 0.59 \cdot COD + 14.31$	0.991	$\Delta I = 0.53 \cdot COD + 11.50$	0.996	$\Delta I = 0.49 \cdot COD + 7.90$	0.996
2.5	$\Delta I = 2.81 \cdot COD + 1{,}933.90$	0.993	$\Delta I = 1.52 \cdot COD + 183.12$	0.997	$\Delta I = 1.35 \cdot COD + 143.18$	0.995
3	$\Delta I = 13.41 \cdot COD + 619.34$	0.992	$\Delta I = 10.86 \cdot COD + 600.29$	0.985	$\Delta I = 8.80 \cdot COD + 459.76$	0.995
3.5	$\Delta I = 13.56 \cdot COD + 1{,}278.68$	0.998	$\Delta I = 11.68 \cdot COD + 994.56$	0.990	$\Delta I = 10.62 \cdot COD + 731.96$	0.982

and 10(e) for the mixed solutions of An/RhB and RhB/KHP, the linear relationship between the ΔI and the COD value was also verified in the range of 5–50 mg/L COD concentration. The related linear equations with about 0.99 correlation coefficients were different for the mixed solutions in different proportions. The increased voltage enhanced the electrocatalytic process significantly. Moreover, the results showed that the net current was not only affected by the types of the organic pollutants but also depended on the volume ratios of the mixed solutions at the same COD concentration. This was because RhB and KHP possessed -COOH groups that inhibited the electrocatalytic degradation of -OH. However, An has the promoting -NH_2 groups.

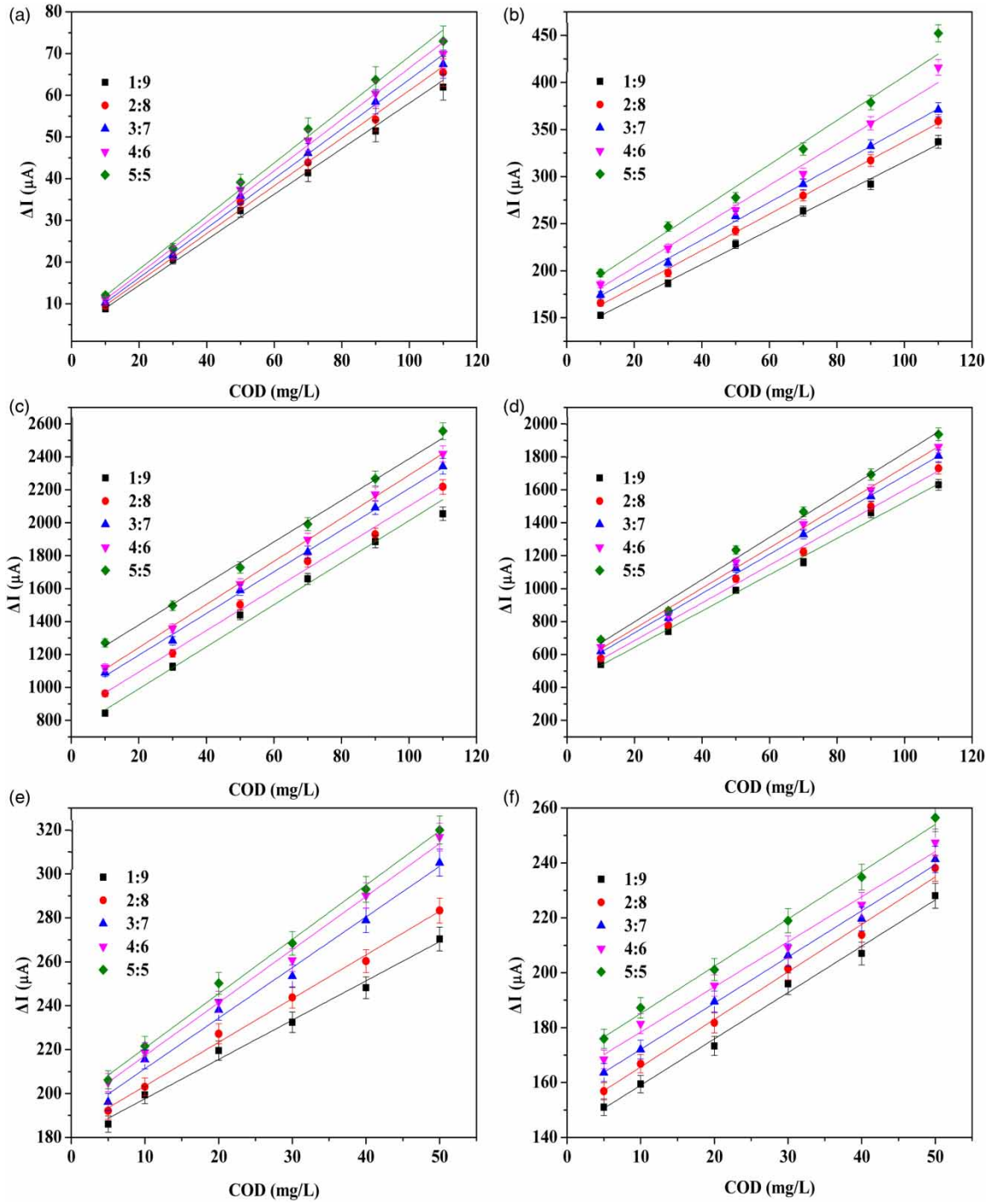

Figure 10 | The linear curves of ΔI and COD of the mixed solutions with different volume ratios of An/KHP at the voltages of 2.0 V (a), 2.5 V (b), 3.0 V (c), and 3.5 V (d); (e) of An/RhB at 2.5 V; and (f) of RhB/KHP at 2.5 V, measured by the Ti/TiO_2 NTA electrode. An, RhB, and KHP stand for aniline, rhodamine B, and potassium hydrogen phthalate, respectively.

According to Equation (4), the promoting groups promoted the consumption of ·OH due to the oxidation of organic matter, while the inhibitory groups were the opposite. Therefore, the specific characteristics of the target organic matter affected the process of generating electrons, thereby affecting the current (Yu *et al.* 2014; Chen *et al.* 2020a; Vaiano *et al.* 2020; Xu *et al.* 2021).

As shown in Figure 11 and Table 5, the net current of the three-component mixed solutions with known COD concentration in the range of 10–110 mg/L was determined by the prepared Ti/TiO_2 NTA electrode. Under a voltage of 2.5 V (vs.

Table 3 | Linear regression equations of net current ΔI and COD value of the two-component solutions of An/KHP

	1:9		2:8		3:7	
An:KHP Voltage (V·vs. SCE)	Linear regression equation (ΔI, μA; COD, mg/L)	R^2	Linear regression equation (ΔI, μA; COD, mg/L)	R^2	Linear regression equation (ΔI, μA; COD, mg/L)	R^2
2	$\Delta I = 0.49 \cdot COD + 9.36$	0.997	$\Delta I = 0.52 \cdot COD + 9.71$	0.997	$\Delta I = 0.54 \cdot COD + 9.90$	0.996
2.5	$\Delta I = 1.82 \cdot COD + 134.49$	0.997	$\Delta I = 1.94 \cdot COD + 143.09$	0.998	$\Delta I = 1.98 \cdot COD + 153.38$	0.998
3	$\Delta I = 11.09 \cdot COD + 420.87$	0.994	$\Delta I = 11.58 \cdot COD + 446.66$	0.996	$\Delta I = 11.93 \cdot COD + 492.89$	0.997
3.5	$\Delta I = 12.18 \cdot COD + 770.28$	0.988	$\Delta I = 12.41 \cdot COD + 852.68$	0.994	$\Delta I = 12.73 \cdot COD + 935.34$	0.997

An:KHP	4:6		5:5	
Voltage (V vs. SCE)	Linear regression equation (ΔI, μA; COD, mg/L)	R^2	Linear regression equation (ΔI, μA; COD, mg/L)	R^2
2	$\Delta I = 0.56 \cdot COD + 10.27$	0.993	$\Delta I = 0.58 \cdot COD + 10.92$	0.993
2.5	$\Delta I = 2.27 \cdot COD + 155.96$	0.989	$\Delta I = 2.45 \cdot COD + 167.29$	0.981
3	$\Delta I = 12.33 \cdot COD + 511.98$	0.995	$\Delta I = 12.83 \cdot COD + 543.83$	0.991
3.5	$\Delta I = 13.11 \cdot COD + 981.85$	0.999	$\Delta I = 12.88 \cdot COD + 1{,}112.49$	0.997

An and KHP stand for aniline and potassium hydrogen phthalate, respectively.

Table 4 | Linear regression equations of net current ΔI and COD value of the two-component solutions of An/RhB and RhB/KHP

	An:RhB		RhB:KHP	
Volume ratios	Linear regression equation (ΔI, μA; COD, mg/L)	R^2	Linear regression equation (ΔI, μA; COD, mg/L)	R^2
1:9	$\Delta I = 1.78 \cdot COD + 180.33$	0.991	$\Delta I = 1.69 \cdot COD + 142.13$	0.993
2:8	$\Delta I = 1.98 \cdot COD + 184.10$	0.994	$\Delta I = 1.74 \cdot COD + 148.27$	0.992
3:7	$\Delta I = 2.30 \cdot COD + 188.58$	0.990	$\Delta I = 1.68 \cdot COD + 155.34$	0.995
4:6	$\Delta I = 2.43 \cdot COD + 193.36$	0.995	$\Delta I = 1.65 \cdot COD + 161.87$	0.990
5:5	$\Delta I = 2.46 \cdot COD + 196.68$	0.995	$\Delta I = 1.72 \cdot COD + 168.05$	0.995

An, RhB, and KHP represent aniline, rhodamine B, and potassium hydrogen phthalate, respectively.

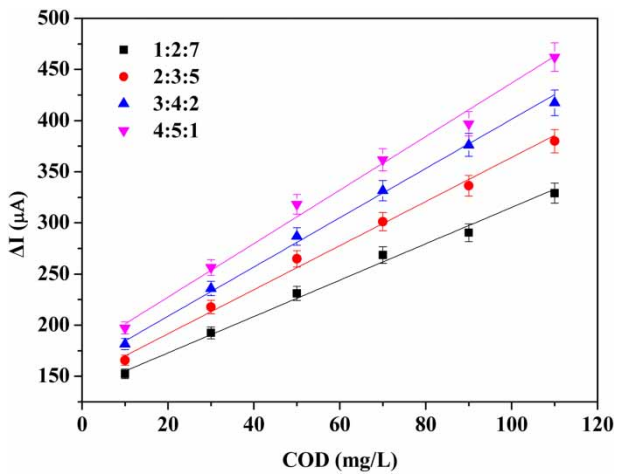

Figure 11 | The linear curves of net current ΔI and COD of the three-component mixed solutions (An/RhB/KHP) at a voltage of 2.5 V on the Ti/TiO_2 NTA electrode. An, RhB, and KHP stand for aniline, rhodamine B, and potassium hydrogen phthalate, respectively.

Table 5 | Linear regression equations of net current ΔI and COD value of the three-component mixed solutions of An/RhB/KHP

Volume ratios (An:RhB:KHP)	Linear regression equation (ΔI, μA; COD, mg/L)	R^2
1:2:7	$\Delta I = 1.73 \cdot COD + 140.37$	0.993
2:3:4	$\Delta I = 2.09 \cdot COD + 152.13$	0.994
3:4:3	$\Delta I = 2.35 \cdot COD + 164.28$	0.996
4:5:1	$\Delta I = 2.55 \cdot COD + 179.96$	0.990

An, RhB, and KHP stand for aniline, rhodamine B, and potassium hydrogen phthalate, respectively.

SCE), there were good linear relationships between ΔI and COD for the three-component solutions with different ratios, and the correlation coefficients were all about 0.99. In addition, the catalytic current was affected by the different volume ratios of the organic solutions. The net current of the An/RhB/KHP solution with a 4:5:1 volume ratio was the largest at the same COD value, while the one with a 1:2:7 volume ratio was the smallest. This was due to the difference in electrochemical reactivity (An > RhB > KHP) and the functional groups of the target organics. Therefore, the linear relationship between ΔI and COD was different for the detection of multi-component mixed solutions of different proportions.

Table 6 summarizes the salient properties of recently developed electrodes for COD detection. The electrode preparation method, target organic solution, operation time, etc. in the comparison table showed that our research has conducted a more

Table 6 | Comparison of the electrodes for COD detection with previously reported literature

Electrode	Preparation method	Detection method	Linearity range (mg/L)	Target substance	Operation time (s)	Reference
Ti/TiO_2 photoelectrode	Laser anneal	Photoelectrocatalysis	50–2,000	S: KHP	> 30	Li *et al.* (2006b)
		Photoelectrocatalysis using flow injection	5–1,000	S: KHP	> 100	Li *et al.* (2007)
Ti/TiO_2/PbO_2 photoelectrode	Dip-coating combined with laser anneal	Photoelectrocatalysis	20–2,500	S: KHP	> 30	Li *et al.* (2006a)
Carbon fiber felt/ β-PbO_2 electrode	Electrochemical deposition	Electrochemical catalysis	50–5,000	S: NaAc, LA, NaCO, Glu, Xyl, HQ, Cys, GmA, p-HbA, p-Np, and KHP	> 120	Mo *et al.* (2015)
Pseudo-graphite electrode	Chemical vapor deposition method	Electrochemical catalysis	0–1 × 10^4	S: Glu, KHP, SDBS, and LA	–	Kabir *et al.* (2019)
Nano-Cu/C electrode	Electrochemical deposition	Electrochemical catalysis	32–256	M: Gly and Glu (ratio of 1:1)	> 120	Diksy *et al.* (2020)
Ti/Sb–SnO_2/PbO_2 composite electrode	Electrochemical deposition	Electrochemical catalysis	0.5–200	S: Glu, Su, Np, HQ, p-HbA, and Te	> 30	Ma *et al.* (2011)
Mixed-phase TiO_2 electrode	Dip-coating	Photoelectrocatalysis	0–200	S and M: KHP, Glu, GrA, SuA, MaA, and Glu-GtA	–	Zhang *et al.* (2009)
Ti/TiO_2 electrode	Anodic oxidation	Electrochemical catalysis	20–2,500	S: KHP	100	Ge *et al.* (2016)
Ti/TiO_2 nanotube array electrode	Secondary anodic oxidation	Electrochemical catalysis	5–150	S and M: An, RhB, and KHP	60	This work

S and M stand for single- and multi-component organic solutions, respectively. An, RhB, and KHP represent aniline, rhodamine B, and potassium hydrogen phthalate, respectively. The similar representative names include: Cys – cysteine, Glu – glucose, Gly – glycine, GmA – glutamic acid, GrA – glutaric acid, HQ – hydroquinone, LA – lactic acid, MaA – malonic acid, NaAc – sodium acetate. $Na_2C_2O_4$ – sodium oxalate, Np – nitrophenol, p-HbA – p-hydroxybenzoic acid, p-Np – p-nitrophenol, Su – sucrose, SuA – succinic acid, SDBS – sodium dodecyl benzenesulfonate, Te – tetracycline, Xyl – xylose.

comprehensive and complete study on COD determination using the prepared Ti/TiO_2 electrode, especially for the detection of single-component and multi-component solutions. Although Zhang *et al.* and Diksy *et al.* mentioned multi-component solutions in their work, they did not conduct in-depth research and discussion on different types and ratios of organic solutions (Zhang *et al.* 2009; Diksy *et al.* 2020). However, this part of the research is of great significance for an actual measurement. In this work, a secondary anodic oxidation method was used to convert Ti electrodes into Ti/TiO_2 nanotube array electrodes with a high-efficiency contact area and multiple active sites. The preparation method is simple and easy to achieve in a short time, without any complex procedures and expensive instruments, compared to the detection method of photoelectrocatalysis (Li *et al.* 2006a, 2006b, 2007; Zhang *et al.* 2009), the instruments for preparation (Li *et al.* 2006a, 2006b, 2007; Zhang *et al.* 2009; Ma *et al.* 2011; Mo *et al.* 2015; Kabir *et al.* 2019; Diksy *et al.* 2020), and the preparation time (Li *et al.* 2006a, 2006b, 2007; Zhang *et al.* 2009; Ma *et al.* 2011; Mo *et al.* 2015; Abdel-Salam *et al.* 2018; Carchi *et al.* 2019; Diksy *et al.* 2020). The effect of the types and ratios of the organics on COD measurement by the Ti/TiO_2 electrode method was studied and discussed in the range of 5–150 mg/L COD. It was revealed that organic compounds with different functional groups influenced electrochemical COD determination. For future research, it is of great significance to improve the work of electrochemical method for COD determination by developing new electrode preparation methods and studying the influence of different types and proportions of organic pollution on the COD measurement results.

In summary, the net current ΔI had a good linear relationship with the COD value of the measurement range for single-, two-, and three-component solutions using the prepared Ti/TiO_2 NTA electrode method, and the correlation coefficients were all about 0.99. In addition, the different linear relationship of each mixed organic solution was due to the electrochemical reactivity. Therefore, under the same COD concentration, the oxidation current of each mixed organic solution was different. This illustrated the difference in the electrocatalytic kinetic behavior of organic substances on the prepared Ti/TiO_2 electrode. Therefore for an early stage of technological applications for Ti/TiO_2 NTA (Zheng *et al.* 2008; Dai *et al.* 2020), advanced fitting methods and preparation methods need to be improved and developed.

4. CONCLUSIONS

In summary, we have demonstrated a COD measurement method based on a prepared Ti/TiO_2 NAT electrode. The Ti/TiO_2 electrode with nanotube array (NTA) structure was prepared by the secondary anodic oxidation method. The composition of the electrode was mainly anatase phase TiO_2, the average inner diameter of the nanotube was ~100 nm, and the wall thickness was ~20 nm. The prepared Ti/TiO_2 NTA electrode was used for electrocatalytic degradation of different organic substances (including An, RhB, and KHP). Thus, the macro-kinetics of the electrocatalytic oxidation of organic compounds on the electrode surface were studied and discussed, conformed to the first-order kinetic reaction. Compared with the electrode reaction activation energy of the organics, the difference in the dynamic behavior of the organic substances on the electrode surface was revealed. Furthermore, using An, RhB, and KHP as target pollutants, the Ti/TiO_2 NTA electrode electrochemical method was used to determine the COD concentration of single-component, two-component, and three-component mixed organic solutions. It was found that the COD value of the solution was directly proportional to the anodizing current, and the correlation coefficients were all about 0.99. It confirmed the feasibility of COD determination of organic solutions using the prepared Ti/TiO_2 electrode. In addition, the oxidation current of the organic substances was different under the same COD concentration, reproving the electrocatalytic kinetic behavior of the organic substances on the electrode surface. Therefore, the oxidation current was related to the COD concentration and the types of organic matter. Furthermore, due to the attractive usability and reusability properties with advantages of simple preparation method, simple detection method, fast detection, expenses reduction, and energy saving for the Ti/TiO_2 NTA electrode, this report offered a feasibility study for COD determination, electrochemical degradation of water pollution, and other electrochemical processes based on Ti/TiO_2 electrodes, especially for detection and monitoring of actual wastewater samples containing organic pollutants.

DATA AVAILABILITY STATEMENT

All relevant data are included in the paper or its Supplementary Information.

REFERENCES

Abdel-Salam, O. E., Abou Taleb, E. M. & Afify, A. A. 2018 Electrochemical treatment of chemical oxygen demand in produced water using flow-by porous graphite electrode. *Water and Environment Journal* **32** (3), 404–411.

Ai, S., Gao, M., Yang, Y., Li, J. & Jin, L. 2004 Electrocatalytic sensor for the determination of chemical oxygen demand using a lead dioxide modified electrode. *Electroanalysis* **16** (5), 404–409.

Carchi, T., Lapo, B., Alvarado, J., Espinoza-Montero, P. J., Llorca, J. & Fernandez, L. 2019 A Nafion film cover to enhance the analytical performance of the CuO/Cu electrochemical sensor for determination of chemical oxygen demand. *Sensors (Basel)* **19** (3), 1–17.

Chen, M., Pan, S., Zhang, C., Wang, C., Zhang, W., Chen, Z., Zhao, X. & Zhao, Y. 2020a Electrochemical oxidation of reverse osmosis concentrates using enhanced TiO_2-NTA/SnO_2-Sb anodes with/without PbO_2 layer. *Chemical Engineering Journal* **399**, 125756.

Chen, S., Li, J., Liu, L., He, Q., Zhou, L., Yang, T., Wang, X., He, P., Zhang, H. & Jia, B. 2020b Fabrication of Co/Pr co-doped Ti/PbO_2 anode for efficiently electrocatalytic degradation of beta-naphthoxyacetic acid. *Chemosphere* **256**, 127139.

Chen, S., Zhou, L., Yang, T., He, Q., Zhou, P., He, P., Dong, F., Zhang, H. & Jia, B. 2020c Thermal decomposition based fabrication of dimensionally stable Ti/SnO_2-RuO_2 anode for highly efficient electrocatalytic degradation of alizarin cyanin Green. *Chemosphere* **261**, 128201.

Chen, Z., Xie, G., Pan, Z., Zhou, X., Lai, W., Zheng, L. & Xu, Y. 2021 A novel Pb/PbO_2 electrodes prepared by the method of thermal oxidation-electrochemical oxidation: characteristic and electrocatalytic oxidation performance. *Journal of Alloys and Compounds* **851**, 156834.

Cheshideh, H. & Nasirpouri, F. 2017 Cyclic voltammetry deposition of nickel nanoparticles on TiO_2 nanotubes and their enhanced properties for electro-oxidation of methanol. *Journal of Electroanalytical Chemistry* **797**, 121–133.

Daghrir, R., Drogui, P., Ka, I. & El Khakani, M. A. 2012 Photoelectrocatalytic degradation of chlortetracycline using Ti/TiO_2 nanostructured electrodes deposited by means of a pulsed laser deposition process. *Journal of Hazardous Materials* **199–200**, 15–24.

Daghrir, R., Drogui, P., Dimboukou-Mpira, A. & El Khakani, M. A. 2013 Photoelectrocatalytic degradation of carbamazepine using Ti/TiO_2 nanostructured electrodes deposited by means of a pulsed laser deposition process. *Chemosphere* **93** (11), 2756–2766.

Dai, Z., Hao, N., Xiong, M., Han, X., Zuo, Y. & Wang, K. 2020 Portable photoelectrochromic visualization sensor for detection of chemical oxygen demand. *Analytical Chemistry* **92** (19), 13604–9.

Diksy, Y., Rahmawati, I., Jiwanti, P. K. & Ivandini, T. A. 2020 Nano-Cu modified Cu and nano-Cu modified graphite electrodes for chemical oxygen demand sensors. *Analytical Sciences* **36** (11), 1323–1330.

Ercin, A. E. & Hoekstra, A. Y. 2014 Water footprint scenarios for 2050: a global analysis. *Environment International* **64**, 71–82.

Garcia-Segura, S., Ocon, J. D. & Chong, M. N. 2018 Electrochemical oxidation remediation of real wastewater effluents – a review. *Process Safety and Environmental Protection* **113**, 48–67.

Ge, Y., Zhai, Y., Niu, D., Wang, Y., Fernandez, C., Ramakrishnappa, T., Hu, X. & Wang, L. 2016 Electrochemical determination of chemical oxygen demand using Ti/TiO_2 electrode. *International Journal of Electrochemical Science* **11**, 9812–9821.

Kabir, H., Zhu, H., Lopez, R., Nicholas, N. W., McIlroy, D. N., Echeverria, E., May, J. & Cheng, I. F. 2019 Electrochemical determination of chemical oxygen demand on functionalized pseudo-graphite electrode. *Journal of Electroanalytical Chemistry* **851**, 113448.

Li, J., Zheng, L., Li, L., Shi, G., Xian, Y. & Jin, L. 2006a Photoelectro-synergistic catalysis at Ti/TiO_2/PbO_2 electrode and its application on determination of chemical oxygen demand. *Electroanalysis* **18** (22), 2251–2256.

Li, J., Zheng, L., Li, L., Shi, G., Xian, Y. & Jin, L. 2006b Ti/TiO_2 electrode preparation using laser anneal and its application to determination of chemical oxygen demand. *Electroanalysis* **18** (10), 1014–1018.

Li, J., Zheng, L., Li, L., Shi, G., Xian, Y. & Jin, L. 2007 Determination of chemical oxygen demand using flow injection with Ti/TiO_2 electrode prepared by laser anneal. *Measurement Science and Technology* **18** (3), 945–951.

Liu, Y., Zhou, B., Bai, J., Li, J., Zhang, J., Zheng, Q., Zhu, X. & Cai, W. 2009 Efficient photochemical water splitting and organic pollutant degradation by highly ordered TiO_2 nanopore arrays. *Applied Catalysis B-Environmental* **89** (1–2), 142–148.

Ma, C., Tan, F., Zhao, H., Chen, S. & Quan, X. 2011 Sensitive amperometric determination of chemical oxygen demand using Ti/Sb–SnO_2/PbO_2 composite electrode. *Sensors and Actuators B: Chemical* **155** (1), 114–119.

Mo, H., Tang, Y., Wang, X., Liu, J., Kong, D., Chen, Y., Wan, P., Cheng, H., Sun, T., Zhang, L., Zhang, M., Liu, S., Sun, Y., Wang, N., Xing, L., Wang, L., Jiang, Y., Xu, X., Zhang, Y. & Meng, X. 2015 Development of a three-dimensional structured carbon fiber felt/β-PbO_2 electrode and its application in chemical oxygen demand determination. *Electrochimica Acta* **176**, 1100–1107.

Ramasundaram, S., Seid, M. G., Lee, W., Kim, C. U., Kim, E. J., Hong, S. W. & Choi, K. J. 2017 Preparation, characterization, and application of TiO_2-patterned polyimide film as a photocatalyst for oxidation of organic contaminants. *Journal of Hazardous Materials* **340**, 300–308.

Saha, P., Bruning, H., Wagner, T. V. & Rijnaarts, H. H. M. 2020 Removal of organic compounds from cooling tower blowdown by electrochemical oxidation: role of electrodes and operational parameters. *Chemosphere* **259**, 127491.

Shannon, M. A., Bohn, P. W., Elimelech, M., Georgiadis, J. G., Marinas, B. J. & Mayes, A. M. 2008 Science and technology for water purification in the coming decades. *Nature* **452** (7185), 301–310.

Shao, C., Zhang, F., Li, X., Zhang, J., Jiang, Y., Cheng, H. & Zhu, K. 2019 Influence of Cr doping on the oxygen evolution potential of SnO_2/Ti and Sb-SnO_2/Ti electrodes. *Journal of Electroanalytical Chemistry* **832**, 436–443.

Silva, C. R., Conceição, C. D. C., Bonifácio, V. G., Filho, O. F. & Teixeira, M. F. S. 2009 Determination of the chemical oxygen demand (COD) using a copper electrode: a clean alternative method. *Journal of Solid State Electrochemistry* **13** (5), 665–669.

Song, M., Cao, H., Zhu, Y., Wang, Y., Zhao, S., Huang, C., Zhang, C. & He, X. 2020 Electrochemical and photocatalytic properties of electrospun C/TiO_2 nanofibers. *Chemical Physics Letters* **747**, 137355.

Tao, J. & Tao, H.-j. 2008 Review of preparation and applications of TiO_2 nanotube arrays. *Machine Building & Automation* **37** (1), 1–4,7.

UNESCO & UN-Water 2020 *United Nations World Water Development Report 2020: Water and Climate Change*. UNESCO, Paris.

Vaiano, V., Sannino, D. & Sacco, O. 2020 Chapter 9 – The use of nanocatalysts (and nanoparticles) for water and wastewater treatment by means of advanced oxidation processes. In: *Nanotechnology in the Beverage Industry* (Amrane, A., Rajendran, S., Nguyen, T. A., Assadi, A. A. & Sharoba, A. M., eds). Elsevier, pp. 241–264.

Wang, H., Wang, J., Bo, G., Wu, S. & Luo, L. 2020 Degradation of pollutants in polluted river water using Ti/IrO_2–Ta_2O_5 coating electrode and evaluation of electrode characteristics. *Journal of Cleaner Production* **273**, 123019.

Xu, T., Song, J., Lin, W., Fu, B., Guo, X., Huang, X., Wu, H. & Zhang, X. 2021 A freestanding carbon submicro fiber sponge as high-efficient bioelectrochemical anode for wastewater energy recovery and treatment. *Applied Energy* **281**, 115913.

Yi, Z., Zeng, Y., Wu, H., Chen, X., Fan, Y., Yang, H., Tang, Y., Yi, Y., Wang, J. & Wu, P. 2019 Synthesis, surface properties, crystal structure and dye-sensitized solar cell performance of TiO_2 nanotube arrays anodized under different parameters. *Results in Physics* **15**, 102609.

Yu, D., Zhu, X., Xu, Z., Zhong, X., Gui, Q., Song, Y., Zhang, S., Chen, X. & Li, D. 2014 Facile method to enhance the adhesion of TiO_2 nanotube arrays to Ti substrate. *ACS Applied Materials & Interfaces* **6** (11), 8001–8005.

Zhang, S., Li, L. & Zhao, H. 2009 A portable photoelectrochemical probe for rapid determination of chemical oxygen demand in wastewaters. *Environmental Science & Technology* **43**, 7810–7815.

Zhang, Y., He, P., Zhou, L., Dong, F., Yang, D., Lei, H., Du, L., Jia, L. & Zhou, S. 2020 Optimized terbium doped Ti/PbO_2 dimensional stable anode as a strong tool for electrocatalytic degradation of imidacloprid waste water. *Ecotoxicology and Environment Safety* **188**, 109921.

Zheng, Q., Zhou, B., Bai, J., Li, L., Jin, Z., Zhang, J., Li, J., Liu, Y., Cai, W. & Zhu, X. 2008 Self-organized TiO_2 nanotube array sensor for the determination of chemical oxygen demand. *Advanced Materials* **20** (5), 1044–1049.

First received 28 January 2021; accepted in revised form 6 July 2021. Available online 19 July 2021